

**Sigma-term form factor of the nucleon in the large- $N_c$  limit**

P. Schweitzer

*Dipartimento di Fisica Nucleare e Teorica, Università degli Studi di Pavia, Pavia, Italy  
and Institut für Theoretische Physik II, Ruhr-Universität Bochum, D-44780 Bochum, Germany*

(Received 9 August 2003; published 20 February 2004)

The scalar isoscalar form factor  $\sigma(t)$  of the nucleon is calculated in the limit of a large number of colors in the framework of the chiral quark-soliton model. The calculation is free of adjustable parameters and based on an approximation justified by the small packing fraction of instantons in the QCD vacuum model, from which the chiral quark-soliton model was derived. The result for  $\sigma(t)$  reproduces all features of the form factor observed in previous exact numerical calculations in the chiral quark-soliton model and in chiral perturbation theory, and agrees well with the available phenomenological information. The Feynman-Hellmann theorem is used to study the pion mass dependence of the nucleon mass and a good agreement with lattice QCD results is observed. The use of the present method to extrapolate lattice data to the chiral limit is discussed.

DOI: 10.1103/PhysRevD.69.034003

PACS number(s): 12.39.Ki, 12.38.Lg, 14.20.Dh

**I. INTRODUCTION**

The pion-nucleon sigma term  $\sigma_{\pi N}$  is of fundamental importance for understanding chiral symmetry breaking effects in the nucleon [1,2]. It can be inferred from pion-nucleon scattering data [3] and the value is found to be  $\sigma_{\pi N} \simeq (50-70)$  MeV [4-9]. The pion-nucleon sigma term has a wide phenomenological impact in many fields. For example, it is related to partial restoration of chiral symmetry in the nuclear medium [10,11] and to central nuclear forces [12]. It is an important ingredient in the mass decomposition of the nucleon [13] and plays an important role in the searches for the Higgs boson [14], dark matter, and supersymmetric particles [15,16]. Valuable insight into the  $\sigma_{\pi N}$  physics was provided from studies in chiral perturbation theory [17-22], lattice QCD [23-25], and numerous chiral models, e.g., Refs. [26-40].

In this paper the scalar isoscalar nucleon form factor  $\sigma(t)$ , which at zero momentum transfer  $t$  yields  $\sigma_{\pi N}$ , is studied in the chiral quark-soliton model ( $\chi$ QSM) [41,42]. The picture of baryons as chiral solitons of the pion field is justified in the limit of a large number of colors  $N_c$  [43]. Despite the fact that in nature  $N_c=3$  does not seem to be large, the  $\chi$ QSM has proven to describe successfully numerous properties of the nucleon [44-47] and to provide valuable insight. E.g., in this model the observation was made of the so-called  $D$  term in generalized parton distribution functions [48]—a fundamental characteristic of the nucleon [49] which, when known, e.g., will provide information about the “distribution of strong forces” in the nucleon [50]. Another recent highlight made on the basis of the soliton picture was the accurate prediction of the exotic  $\Theta^+$  baryon [51] for which by now strong experimental indications have been collected [52].

The  $\chi$ QSM was derived from the instanton model of the QCD vacuum [53,54] and incorporates chiral symmetry breaking. The field theoretical character of the model plays a crucial role in ensuring the theoretical consistency of the approach. Both  $\sigma_{\pi N}$  and  $\sigma(t)$  were already studied in the  $\chi$ QSM in Refs. [27-29], where the model expressions were exactly evaluated using involved numerical methods. Instead

the calculation of  $\sigma(t)$  presented here is based on an approximation which is consistently justified by arguments from the instanton vacuum model.

The approximate method not only considerably simplifies the calculation—allowing a lucid interpretation of the results and suggesting an appealing explanation why  $\sigma_{\pi N}$  is so large. In addition it has methodical advantages over the exact calculations [27-29]. For in the  $\chi$ QSM  $\sigma(t)$  is quadratically UV divergent and as such strongly sensitive to the details of regularization. The virtue of the approximate method is that it yields a regularization scheme independent result. Another advantage is that the theoretical accuracy of the results—which in models often has to be concluded from the comparison to phenomenology—is here known in advance and under theoretical control. To within this accuracy results from the exact  $\chi$ QSM calculations [27-29] are reproduced, and a good agreement with phenomenological information and results from other approaches is observed without any adjustable parameters.

Another advantage is that the approximation allows us to analytically study the properties of  $\sigma(t)$  in the chiral limit—which is a rare occasion in the  $\chi$ QSM. Finally, by exploring the Feynman-Hellmann theorem [55], the pion mass ( $m_\pi$ ) dependence of the nucleon mass ( $M_N$ ) is studied. An exact treatment of this issue in the  $\chi$ QSM would be numerically highly involved. The results for  $M_N(m_\pi)$  compare well to lattice QCD results. This observation could be used to inspire *Ansätze* for the chiral extrapolation of lattice data.

This paper is organized as follows. In Sec. II the form factor  $\sigma(t)$  is defined and briefly discussed. In Sec. III the model is introduced. The form factor is computed in Sec. IV and the numerical results are discussed in Sec. V. Section VI is devoted to the study of  $\sigma(t)$  and the nucleon mass as functions of the pion mass. Section VII contains the conclusions. Technical details of the calculation can be found in Appendixes A and B.

**II. SCALAR ISOSCALAR NUCLEON FORM FACTOR**

The nucleon sigma-term form factor  $\sigma(t)$  is defined as the form factor of the double commutator of the strong interac-

tion Hamiltonian with two axial isovector charges [1]. Disregarding a “double isospin violating term” proportional to  $(m_u - m_d)(\bar{\psi}_u \psi_u - \bar{\psi}_d \psi_d)$  and commonly presumed to be negligible the form factor can be expressed as

$$\sigma(t) \bar{u}(\mathbf{p}') u(\mathbf{p}) = m \langle N(\mathbf{p}') | [\bar{\psi}_u(0) \psi_u(0) + \bar{\psi}_d(0) \psi_d(0)] | N(\mathbf{p}) \rangle, \quad t = (p - p')^2, \quad (1)$$

where  $m = \frac{1}{2}(m_u + m_d)$ . In Eq. (1)  $|N(\mathbf{p})\rangle$  is the spin-averaged state of the nucleon of momentum  $\mathbf{p}$  normalized as  $\langle N(\mathbf{p}') | N(\mathbf{p}) \rangle = 2p^0 \delta^{(3)}(\mathbf{p} - \mathbf{p}')$ , and  $u(\mathbf{p})$  is the nucleon spinor with  $\bar{u}(\mathbf{p}) u(\mathbf{p}) = 2M_N$ .

At zero-momentum transfer the form factor yields the pion-nucleon sigma term, i.e.,

$$\sigma_{\pi N} \equiv \sigma(0) = \frac{m}{2M_N} \langle N(\mathbf{p}) | [\bar{\psi}_u(0) \psi_u(0) + \bar{\psi}_d(0) \psi_d(0)] | N(\mathbf{p}) \rangle. \quad (2)$$

The pion-nucleon sigma term  $\sigma_{\pi N}$  is normalization scale invariant. The form factor  $\sigma(t)$  describes the elastic scattering off the nucleon due to the exchange of an isoscalar spin-zero particle. It is not known experimentally except for its value at the (unphysical) Cheng-Dashen point  $t = 2m_\pi^2$ . A low-energy theorem [3] relates the value of  $\sigma(t)$  at the so-called Cheng-Dashen point  $t = 2m_\pi^2$  to the (isoscalar even) pion-nucleon scattering amplitude. The analysis of pion-nucleon scattering data yields

$$\sigma(2m_\pi^2) = \begin{cases} (64 \pm 8) \text{ MeV} & (1982) [4] \\ (88 \pm 15) \text{ MeV} & (1999) [6] \\ (71 \pm 9) \text{ MeV} & (1999) [7] \\ (79 \pm 7) \text{ MeV} & (2001) [8]. \end{cases} \quad (3)$$

The recent analyses tend to yield a larger value for  $\sigma(2m_\pi^2)$  which can be explained by the more recent and accurate data [9]. The difference  $\sigma(2m_\pi^2) - \sigma(0)$  has been calculated from a dispersion relation analysis [5],

$$\sigma(2m_\pi^2) - \sigma(0) = (15.2 \pm 0.4) \text{ MeV}. \quad (4)$$

In Ref. [21] a similar result was obtained from a calculation in the chiral perturbation theory. From Eqs. (3),(4) one concludes

$$\sigma_{\pi N} \approx (50 - 70) \text{ MeV}. \quad (5)$$

The large value of  $\sigma_{\pi N}$  has been and still is a puzzle [1,2].

According to the “standard interpretation”  $\sigma_{\pi N}$  can be related to the so-called strangeness content  $y \equiv 2 \langle N | \bar{\psi}_s \psi_s | N \rangle / \langle N | (\bar{\psi}_u \psi_u + \bar{\psi}_d \psi_d) | N \rangle$  of the nucleon as  $(1 - y) \sigma_{\pi N} = \hat{\sigma}$ , where  $\hat{\sigma}$  can be determined by means of chiral perturbation theory from baryon mass splittings,  $\hat{\sigma} = (35 \pm 5) \text{ MeV}$  [17,56]. The value in Eq. (5) then implies  $y \sim (0.3 - 0.4)$  while one would expect  $y \sim 0$  on the grounds of

the Okubo–Zweig–Iizuka (OZI) rule. It is worthwhile mentioning that such a sizeable value of  $y$  naturally follows from a Goldstone-boson-pair mechanism [26].

### III. CHIRAL QUARK SOLITON MODEL ( $\chi$ QSM)

This section briefly introduces the notions required in the following. More complete presentations of the model can be found in, e.g., Refs. [27,41,42]. The  $\chi$ QSM is based on the effective chiral relativistic quantum field theory of quarks, antiquarks, and Goldstone bosons defined by the partition function [54,57,58]

$$Z_{\text{eff}} = \int \mathcal{D}\psi \mathcal{D}\bar{\psi} \mathcal{D}U \exp \left( i \int d^4x \bar{\psi} (i \not{D} - M U \gamma_5 - m) \psi \right), \quad (6)$$

$$U = \exp(i \tau^a \pi^a),$$

$$U \gamma_5 = \exp(i \gamma_5 \tau^a \pi^a) = \frac{1}{2} (U + U^\dagger) + \frac{1}{2} (U - U^\dagger) \gamma_5.$$

In Eq. (6)  $M$  is the dynamical quark mass, which is due to spontaneous breakdown of chiral symmetry and in general momentum dependent.  $U = \exp(i \tau^a \pi^a)$  denotes the SU(2) chiral pion field and  $m$  the current quark mass, which explicitly breaks the chiral symmetry. In many applications  $m$  can be set to zero, but for certain quantities it is convenient or even necessary to consider finite  $m$ . The effective theory (6) contains the Wess-Zumino term and the four-derivative Gasser-Leutwyler terms with correct coefficients [42]. It has been derived from the instanton model of the QCD vacuum [53,54] and is valid at low energies below a scale set by the inverse of the average instanton size

$$\rho_{\text{av}}^{-1} \approx 600 \text{ MeV}. \quad (7)$$

In practical calculations it is convenient to take the momentum dependent quark mass constant, i.e.,  $M(p) \rightarrow M(0) = 350 \text{ MeV}$ . In this case  $\rho_{\text{av}}^{-1}$  is to be understood as the cutoff, at which quark momenta have to be cut off within some appropriate regularization scheme.

It is important to remark that  $(M \rho_{\text{av}})^2$  is proportional to the parametrically small instanton packing fraction, i.e., with  $R_{\text{av}}$  denoting the average distance between instantons in Euclidean space-time,

$$(M \rho_{\text{av}})^2 \propto \left( \frac{\rho_{\text{av}}}{R_{\text{av}}} \right)^4 \ll 1. \quad (8)$$

Numerically  $\rho_{\text{av}}/R_{\text{av}} \sim 1/3$ . The parameterical smallness of this quantity played an important role in the derivation of the effective theory (6) from the instanton model of the QCD vacuum [41,53].

The  $\chi$ QSM is an application of the effective theory (6) to the description of baryons [41,42]. The large- $N_c$  limit allows to solve the path integral over pion field configurations in Eq. (6) in the saddle-point approximation. In the leading order of

the large- $N_c$  limit the pion field is static, and one can determine the spectrum of the one-particle Hamiltonian of the effective theory (6),

$$\hat{H}|n\rangle = E_n|n\rangle, \quad \hat{H} = -i\gamma^0\gamma^k\partial_k + \gamma^0 M U^{\gamma_5} + \gamma^0 m. \quad (9)$$

The spectrum consists of an upper and a lower Dirac continuum, distorted by the pion field as compared to continua of the free Dirac-Hamiltonian,

$$\hat{H}_0|n_0\rangle = E_{n_0}|n_0\rangle, \quad \hat{H}_0 = -i\gamma^0\gamma^k\partial_k + \gamma^0 M + \gamma^0 m, \quad (10)$$

and of a discrete bound-state level of energy  $E_{\text{lev}}$ , if the pion field is strong enough. By occupying the discrete level and the states of the lower continuum each by  $N_c$  quarks in an antisymmetric color state, one obtains a state with unity baryon number. The soliton energy  $E_{\text{sol}}$  is a functional of the pion field,

$$E_{\text{sol}}[U] = N_c \left( E_{\text{lev}} + \sum_{E_n < 0} (E_n - E_{n_0}) \right) \Big|_{\text{reg}}. \quad (11)$$

$E_{\text{sol}}[U]$  is logarithmically divergent and has to be regularized appropriately, which is indicated in Eq. (11). Minimization of  $E_{\text{sol}}[U]$  determines the self-consistent solitonic pion field  $U_c$ . This procedure is performed for symmetry reasons in the so-called hedgehog *Ansatz*,

$$\pi^a(\mathbf{x}) = e_r^a P(r), \quad U(\mathbf{x}) = \cos P(r) + i\tau^a e_r^a \sin P(r), \quad (12)$$

with the radial (soliton profile) function  $P(r)$  and  $r = |\mathbf{x}|$ ,  $\mathbf{e}_r = \mathbf{x}/r$ . The nucleon mass  $M_N$  is given by  $E_{\text{sol}}[U_c]$ . The momentum and the spin and isospin quantum numbers of the baryon are described by considering zero modes of the soliton. Corrections in the  $1/N_c$ -expansion can be included by considering time-dependent pion field fluctuations around the solitonic solution. The  $\chi$ QSM provides a practical realization of the large- $N_c$  picture of the nucleon [43].

The self-consistent profile satisfies  $P_c(0) = -\pi$  and decays in the chiral limit as  $1/r^2$  at large  $r$ . For finite  $m$  it exhibits a Yukawa tail  $\propto \exp(-m_\pi r)/r$  with the pion mass  $m_\pi$  connected to  $m$  by the Gell-Mann–Oakes–Renner relation; see below, Eq. (34). An excellent approximation to the self-consistent profile, which exhibits all those features (and is sufficient for our purposes) is given by the analytical ‘‘arctan-profile,’’

$$P(r) = -2 \arctan \left( \frac{R_{\text{sol}}^2}{r^2} (1 + m_\pi r) e^{-m_\pi r} \right), \quad R_{\text{sol}} = M^{-1}. \quad (13)$$

The quantity  $R_{\text{sol}}$  is referred to as the soliton size. It is related to the nucleon axial coupling constant  $g_A = 1.25$  as [42,59] (note that the order of the limits cannot be inversed)

$$\lim_{r \rightarrow \infty} \left( \lim_{m_\pi \rightarrow 0} r^2 P(r) \right) = -2R_{\text{sol}}^2 = -\frac{3}{8\pi} \frac{g_A}{f_\pi^2}. \quad (14)$$

The  $\chi$ QSM allows us to evaluate without adjustable parameters nucleon matrix elements of QCD quark bilinear operators as

$$\begin{aligned} & \langle N(\mathbf{p}') | \bar{\psi}(0) \Gamma \psi(0) | N(\mathbf{p}) \rangle \\ &= c_\Gamma M_N N_c \sum_{n, \text{occ}} \int d^3\mathbf{x} e^{i(\mathbf{p}' - \mathbf{p})\mathbf{x}} \Phi_n(\mathbf{x}) \Gamma \Phi_n(\mathbf{x}) \Big|_{\text{reg}} + \dots, \end{aligned} \quad (15)$$

where  $\Gamma$  is some Dirac and flavor matrix,  $c_\Gamma$  is a constant depending on  $\Gamma$  and the spin and flavor quantum numbers of the nucleon state  $|N\rangle = |S_3, T_3\rangle$ , and  $\Phi_n(\mathbf{x}) = \langle \mathbf{x} | n \rangle$  are the coordinate space wave functions of the single quark states  $|n\rangle$  defined in Eq. (9). The sum in Eq. (15) goes over occupied levels  $n$  (i.e.,  $n$  with  $E_n \leq E_{\text{lev}}$ ), and vacuum subtraction is implied for  $E_n < E_{\text{lev}}$  analog to Eq. (11). The dots denote terms subleading in the  $1/N_c$  expansion (which can be included but will not be considered in this work). The model expressions can contain UV divergences which have to be regularized as indicated in Eq. (15).

If in QCD the quantity on the left-hand side of Eq. (15) is normalization scale dependent, the model result refers to a scale of  $\mathcal{O}(\rho_{\text{av}}^{-1})$ , see Eq. (7). In the way sketched in Eq. (15) a large variety of static nucleon properties like form factors, axial properties, etc., were computed (see Refs. [44,45] for reviews). In Ref. [46] the approach was generalized to non-local quark bilinear operators on the left-hand side of Eq. (15) which paved the way to the study of the quark and antiquark distribution functions [46,47] and off-forward distribution functions [48]. The model results agree typically to within (10–30) % with experimental data or phenomenological information.

#### IV. $\sigma(t)$ IN THE $\chi$ QSM

In this section first the model expression for  $\sigma(t)$  is discussed and the consistency of the approach is demonstrated. Next the UV behavior of  $\sigma(t)$  is studied and the question of regularization is addressed. Thereby is defined and justified the approximation in which then  $\sigma(t)$  is evaluated in the following Section V.

*Expression and consistency.* The pion-nucleon sigma term  $\sigma_{\pi N}$  was studied in the framework of the  $\chi$ QSM in Refs. [27,28] and the scalar isoscalar form factor  $\sigma(t)$  in Ref. [29]. In leading order of the large- $N_c$  limit the model expression for the form factor  $\sigma(t)$  reads [29] [in the SU(2) flavor sector]

$$\sigma(t) = m N_c \int d^3\mathbf{x} j_0(\sqrt{-t}|\mathbf{x}|) \sum_{n, \text{occ}} \Phi_n^*(\mathbf{x}) \gamma^0 \Phi_n(\mathbf{x}) \Big|_{\text{reg}}, \quad (16)$$

where the Bessel function  $j_0(z) = \sin z/z$ . In the large- $N_c$  limit the nucleon mass  $M_N = \mathcal{O}(N_c)$  while the nucleon momenta  $|\mathbf{p}|$  and  $|\mathbf{p}'| = \mathcal{O}(N_c^0)$  such that  $t = -(\mathbf{p}' - \mathbf{p})^2$ . Therefore Eq. (16) is valid for  $|t| \ll M_N^2$ . (Interestingly, in the case of electromagnetic form factors the model results agree well

with data up to  $|t| \sim 1 \text{ GeV}^2$  [44].) Equation (16) shows that  $\sigma(t) = \mathcal{O}(N_c)$  in agreement with results from large- $N_c$  chiral perturbation theory [22].

In the  $\chi$ QSM one is in a position to derive the model expression for  $\sigma_{\pi N}$  in three different ways:

$$\sigma_{\pi N} = \lim_{t \rightarrow 0} \sigma(t), \quad (17)$$

$$\sigma_{\pi N} = m \frac{\partial M_N(m)}{\partial m}, \quad (18)$$

$$\sigma_{\pi N} = m \int_0^1 dx (e^u + e^d + e^{\bar{u}} + e^{\bar{d}})(x). \quad (19)$$

The first method (17) consists in continuing analytically the form factor  $\sigma(t)$  to  $t=0$ . The second method (18) uses the Feynman-Hellmann theorem [55]. The third method (19) uses the sum rule for the first moment of the flavor singlet twist-3 chirally odd distribution function  $e^a(x)$  [60].<sup>1</sup> The three methods consistently yield

$$\sigma_{\pi N} = m N_c \int d^3 \mathbf{x} \sum_{n, \text{occ}} \Phi_n^*(\mathbf{x}) \gamma^0 \Phi_n(\mathbf{x}) \Big|_{\text{reg}}. \quad (20)$$

The result in Eq. (20) immediately follows from the model expression (16) [recalling  $j_0(z) \rightarrow 1$  for  $z \rightarrow 0$ ]. Relation (18) was used to numerically compute  $\sigma_{\pi N}$  in Ref. [27], and explicitly demonstrated to yield the expression in Eq. (20) in Ref. [62]. The sum rule (19) was shown to be satisfied in the  $\chi$ QSM [and to yield Eq. (20) for  $\sigma_{\pi N}$ ] in Refs. [62,63]. The fact that  $\sigma_{\pi N}$  can consistently be computed in the  $\chi$ QSM in three different ways illustrates the theoretical consistency of the model.

*The UV behavior of  $\sigma(t)$ .* In this paragraph the known result, cf. Refs. [27–29], will be rederived that the model expression for  $\sigma(t)$  contains quadratic and logarithmic divergences, i.e., that it is of the form

$$\sigma(t) = a_2(t) \left( \frac{\Lambda_{\text{cut}}}{M} \right)_{\text{reg}}^2 + a_{\log}(t) \log \left( \frac{\Lambda_{\text{cut}}}{M} \right)_{\text{reg}} + a_0(t) \left( \frac{\Lambda_{\text{cut}}}{M} \right)^0, \quad (21)$$

where the coefficients  $a_i(t)$  are UV-finite functions of  $t$  and  $\Lambda_{\text{cut}}$  is an UV cutoff. A similar study was presented in Ref. [62], however, for the more involved case of the twist-3 distribution function  $e^a(x)$  which is related to  $\sigma_{\pi N}$  by means of the sum rule (19).

Let us separately consider the contributions from the discrete level and the negative continuum

$$\sigma(t) = \sigma(t)_{\text{lev}} + \sigma(t)_{\text{cont}},$$

$$\sigma(t)_{\text{lev}} = m N_c \int d^3 \mathbf{x} j_0(\sqrt{-t}|\mathbf{x}|) \Phi_{\text{lev}}^*(\mathbf{x}) \gamma^0 \Phi_{\text{lev}}(\mathbf{x}), \quad (22)$$

$$\sigma(t)_{\text{cont}} = m N_c \int d^3 \mathbf{x} j_0(\sqrt{-t}|\mathbf{x}|) \sum_{E_n < 0} \Phi_n^*(\mathbf{x}) \gamma^0 \Phi_n(\mathbf{x}) \Big|_{\text{reg}}. \quad (23)$$

For the discrete level the eigenvalue problem  $\hat{H} \Phi_{\text{lev}}(\mathbf{x}) = E_{\text{lev}} \Phi_{\text{lev}}(\mathbf{x})$  can exactly be solved numerically, see, e.g., Ref. [46], and with  $\Phi_{\text{lev}}(\mathbf{x})$  one obtains  $\sigma(t)_{\text{lev}}$ . The contribution of the discrete level is always finite and for our purposes it is sufficient to note

$$\sigma(t)_{\text{lev}} = \text{UV finite}. \quad (24)$$

The exact evaluation of the continuum contribution in Ref. (23) is far more involved. For that one either can place the soliton in a finite 3D box, discretize and make finite the spectrum of the free Hamiltonian (10) by imposing boundary conditions and diagonalize the Hamiltonian (9) in the basis of the free Hamiltonian states (Kahana-Ripka method [64]). Alternatively one can rewrite the continuum contribution (23) in terms of Green functions and evaluate those by means of phase shift methods (see, e.g., Ref. [65]). Both methods are numerically involved.

Here we will use an approximate method—referred to as the *interpolation formula* in Ref. [46]—which consists in expanding the continuum contribution (23) in gradients of the  $U$  field and retaining the leading order only. The interpolation formula yields exact results in three limiting cases  $|\nabla U| \ll M$ ,  $|\nabla U| \gg M$ , and  $|\log U| \ll 1$ . Therefore one can expect that it yields useful estimates also for the general case. It was observed that this method approximates exact calculations in the model with good accuracy [46,47].

Let us rewrite the continuum contribution in Eq. (23) (recalling the implicit vacuum subtraction) as

$$\sigma(t)_{\text{cont}} = m N_c \int_C \frac{d\omega}{2\pi i} \text{Sp} \left[ j_0(\sqrt{-t}|\hat{\mathbf{x}}|) \gamma^0 \frac{1}{\omega + i\hat{H}} - (\hat{H} \rightarrow \hat{H}_0) \right]_{\text{reg}}, \quad (25)$$

where the contour  $C$  is defined as going along the real  $\omega$  axis and closed in the infinity in the upper half of the complex  $\omega$  plane. The original expression (23) is recovered by saturating the functional trace with the complete set of eigenfunctions of respectively  $\hat{H}$  and  $\hat{H}_0$  in Eqs. (9),(10),<sup>2</sup> performing the  $\omega$  integration, and passing to the coordinate space representation. Expanding Eq. (25) in a series in gradients of the  $U$  field,

<sup>2</sup>I.e.,  $\text{Sp}[\dots - (\hat{H} \rightarrow \hat{H}_0)] \equiv \sum_{\text{all } n} \langle n | \dots | n \rangle - \sum_{\text{all } n_0} \langle n_0 | \dots | n_0 \rangle$ .

<sup>1</sup>Equation (19) is correct in a formal mathematical sense [60]. However, the sum rule (19) is saturated by a  $\delta$  function at  $x=0$  in  $e^a(x)$  which means that the relation (19) is practically useless to extract any information on  $\sigma_{\pi N}$  from possible measurements of  $e^a(x)$  in deeply inelastic scattering experiments, see Ref. [61] and references therein.

$$\sigma(t)_{\text{cont}} = \sum_{k=0}^{\infty} \sigma(t)_{\text{cont}}^{(k)}, \quad (26)$$

where the index  $k$  means that  $\nabla U$  appears  $k$  times in  $\sigma(t)_{\text{cont}}^{(k)}$ , we obtain (see Appendix A)

$$\sigma(t)_{\text{cont}}^{(k)} = \begin{cases} \alpha B(t) & \text{for } k=0, \\ \text{zero} & \text{for } k=1, \\ \text{UV-finite} & \text{for } k \geq 2, \end{cases} \quad (27)$$

with the constant  $\alpha$  and the ‘‘form factor’’  $B(t)$  defined as

$$\alpha = m \int \frac{d^4 p_E}{(2\pi)^4} \frac{8N_c M}{p_E^2 + M^2} \Big|_{\text{reg}}, \quad (28)$$

$$B(t) = \int d^3 \mathbf{x} j_0(\sqrt{-t}|\mathbf{x}|) \left( 1 - \frac{1}{2} \text{tr}_F U(\mathbf{x}) \right). \quad (29)$$

The factor  $8N_c M m$  is included into the definition of  $\alpha$  for later convenience. The Euclidean integral in the constant  $\alpha$  contains quadratic and logarithmic divergences. Combining the results in Eq. (24) and Eqs. (27), (29) we see that the form factor  $\sigma(t)$  has the UV behavior (21) [and that  $a_2(t) \propto a_{\log}(t) \propto B(t)$ ].

*Instanton motivated approximation.* In nonrenormalizable effective (low energy) theories the regularization procedure ‘‘keeps the memory’’ of the cutoff  $\Lambda_{\text{cut}}$ . In such effective theories—for which Eq. (6) is an example—the cutoff has a physical meaning: It sets the scale below which the degrees of freedom of the effective theory may be considered as appropriate to describe the physical situation, and above which they may not be sufficient. In the effective theory (6) the cutoff

$$\Lambda_{\text{cut}} = \mathcal{O}(\rho_{\text{av}}^{-1}). \quad (30)$$

Using Eq. (30) and the results of the previous paragraph we see that  $\sigma(t)$  can be written as

$$\sigma(t) = \alpha B(t) \cdot \{1 + \mathcal{O}(M^2 \rho_{\text{av}}^2)\} \quad (31)$$

with  $\alpha$  and  $B(t)$  as defined in Eqs. (28),(29).

Thus in Eq. (21) the UV-finite contributions are parametrically strongly suppressed with respect to the UV-divergent terms by the instanton packing fraction due to Eq. (8). Since the  $\chi$ QSM was derived from the instanton vacuum model, it is consistent to use this argument based on Eqs. (8),(30) in this context. Equation (31) defines the approximation in which  $\sigma(t)$  will finally be evaluated, after regularizing the divergent constant  $\alpha$  in Eq. (28).

*Regularization.* There are several methods to regularize the divergent constant  $\alpha$  in Eq. (28). Popular methods often used in exact model calculations are the Schwinger proper-time regularization (see, e.g., Ref. [44]) or the Pauli-Villars subtraction method (see, e.g., Refs. [62,66]). The result will be sensitive to the chosen regularization method and, espe-

cially for a power divergent quantity, to the precise value of the cutoff—of which only the order of magnitude is known, cf. Eq. (30).

However, the practical problem of how to regularize the constant  $\alpha$  in Eq. (28) can be solved elegantly and in a regularization independent way. Since the quark vacuum condensate  $\langle \bar{\psi}\psi \rangle_{\text{vac}}$  is given in the effective theory (6) by [54]

$$\begin{aligned} \langle \bar{\psi}\psi \rangle_{\text{vac}} &\equiv \langle \text{vac} | [\bar{\psi}_u(0)\psi_u(0) + \bar{\psi}_d(0)\psi_d(0)] | \text{vac} \rangle \\ &= \int \frac{d^4 p_E}{(2\pi)^4} \frac{(-8N_c M)}{p_E^2 + M^2} \Big|_{\text{reg}}, \end{aligned} \quad (32)$$

the constant  $\alpha$  in Eq. (28) can be expressed as

$$\alpha = -m \langle \bar{\psi}\psi \rangle_{\text{vac}}. \quad (33)$$

At first glance Eq. (33) is based on the mere observation that the same divergent integral appears in two different model expressions. However, as will be discussed in the next section, the relation (33) is not accidental from a physical point of view (and implies an interesting interpretation of  $\sigma_{\pi N}$ ). In the next step one can use the Gell-Mann–Oakes–Renner relation (with  $f_\pi$  denoting the pion decay constant)

$$m_\pi^2 f_\pi^2 = -m \langle \bar{\psi}\psi \rangle_{\text{vac}}, \quad (34)$$

which is not imposed here by hand but valid in the effective theory (6) [54]. Thanks to Eqs. (33),(34) the practical problem of regularizing  $\sigma(t)$  is shifted to the problem of regularizing  $\langle \bar{\psi}\psi \rangle_{\text{vac}}$  in Eq. (32) or  $f_\pi$ . The latter is given in the effective theory (6) by the logarithmically UV-divergent expression [54]

$$f_\pi^2 = \int \frac{d^4 p_E}{(2\pi)^4} \frac{4N_c M^2}{(p_E^2 + M^2)^2} \Big|_{\text{reg}}. \quad (35)$$

Since the precise value of the cutoff is not known but only its order of magnitude, see Eq. (7), it is customary to adjust the cutoff(s) in the corresponding regularization scheme such that the experimental values of  $\langle \bar{\psi}\psi \rangle_{\text{vac}}$  and  $f_\pi$  in Eqs. (32,35) are reproduced [44]. In this way free parameters (cutoff, current quark mass, etc.) are fixed in the vacuum and meson sector of the effective theory (6) [44]. In this sense the  $\chi$ QSM—i.e., the baryon sector of the effective theory (6)—yields parameter-free results. [In some calculations in the  $\chi$ QSM the mass  $M$  was understood as a ‘‘free parameter’’ and allowed to vary in the range  $350 \leq M \leq 450$  MeV [28,29,44]. The sensitivity of the model results to these variations was typically within (10–30)%. Here we rely on notions from the instanton vacuum model and consequently take the value  $M = 350$  MeV which follows from the instanton phenomenology [53,54].]

Thus our final (regularized) result for the form factor reads [with  $B(t)$  defined in Eq. (29)]

$$\sigma(t) = m_\pi^2 f_\pi^2 B(t) \cdot \{1 + \mathcal{O}(M^2 \rho_{\text{av}}^2)\}, \quad (36)$$

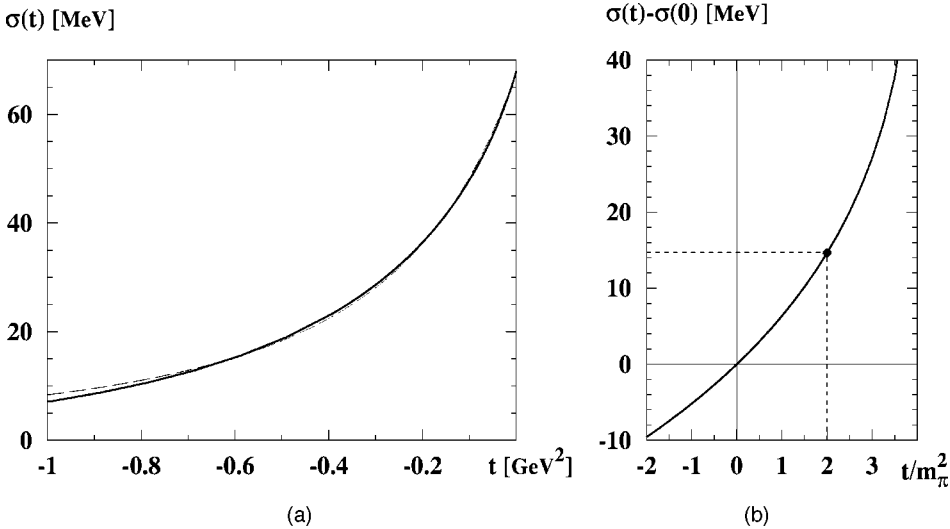


FIG. 1. (a) The form factor  $\sigma(t)$  evaluated in the  $\chi$ QSM by means of Eq. (36) (solid line) and its dipole fit (42) as functions of  $t$ . (b) The analytical continuation of the form factor  $\sigma(t)$  to unphysical  $t \geq 0$ . The dot marks the value of  $\sigma(t)$  at the Cheng-Dashen point  $t = 2m_\pi^2$ . At and above the threshold  $t \geq 4m_\pi^2$  the form factor is not defined, see text.

where  $m_\pi$  and  $f_\pi$  denote the physical pion mass and decay constant, respectively. It should be stressed that the result (36) does not follow from the interpolation formula of Ref. [46] (which would require to add the UV-finite discrete level contribution, cf. Ref. [62]). Instead Eq. (36) has to be considered as an approximate result for  $\sigma(t)$  in the  $\chi$ QSM, which is justified by the parametrical smallness of the instanton packing fraction.

In the following the parametrically small  $\mathcal{O}(M^2 \rho_{av}^2)$  corrections often will not be indicated.

### V. DISCUSSION AND INTERPRETATION OF THE RESULTS

Evaluating the final expression (36) for the form factor  $\sigma(t)$  with the soliton profile (13) for  $M = 350$  MeV,  $m_\pi = 140$  MeV, and  $f_\pi = 93$  MeV yields the result shown in Figs. 1(a) and (b) (see Appendix B for detailed expressions). It should be noted that the error due to using the profile (13), instead of the self-consistent profile which truly minimizes the soliton energy (11), is far smaller than the theoretical accuracy in Eq. (36).

Apart from the values of  $\sigma(t)$  at the Cheng-Dashen point  $t = 2m_\pi^2$  and at  $t = 0$ , and their difference  $\Delta_\sigma = \sigma(2m_\pi^2) - \sigma(0)$ , there is another phenomenologically interesting quantity—namely the scalar mean square radius related to the slope of the form factor  $\sigma(t)$  at  $t = 0$  as

$$\sigma(t) = \sigma_{\pi N} \left( 1 + \frac{1}{6} \langle r_S^2 \rangle t + \mathcal{O}(t^2) \right). \quad (37)$$

We obtain the results

$$\sigma_{\pi N} = 67.9 \text{ MeV}, \quad (38)$$

$$\sigma(2m_\pi^2) = 82.6 \text{ MeV}, \quad (39)$$

$$\Delta_\sigma = 14.7 \text{ MeV}, \quad (40)$$

$$\langle r_S^2 \rangle = 1.00 \text{ fm}^2. \quad (41)$$

A useful parametrization of the form factor for negative  $t$  is given by [with  $\sigma_{\pi N}$  from Eq. (38)]

$$\sigma(t) \approx \frac{\sigma_{\pi N}}{(1 - t/M_S^2)^2}, \quad M_S^2 \approx 0.55 \text{ GeV}^2. \quad (42)$$

The dipole fit (42) approximates  $\sigma(t)$  to within 2% for  $|t| \leq 0.8 \text{ GeV}^2$ , cf. Fig. 1(a). Thus  $\sigma(t)$  decreases with increasing  $|t|$  more quickly than the electromagnetic form factors where the corresponding dipole mass is about  $M_{em}^2 \sim 0.7 \text{ GeV}^2$  in a comparable  $t$  region.

The form factor  $\sigma(t)$ , Eq. (36), is not defined at and above the threshold  $t \geq 4m_\pi^2$ . In the vicinity of the threshold the form factor behaves as (see Appendix B)

$$\sigma(t) = a_1 \ln \left( \frac{1}{1 - \frac{\sqrt{t}}{2m_\pi}} \right) + a_2 \text{ as } t \rightarrow 4m_\pi^2 \quad (t < 4m_\pi^2), \quad (43)$$

where  $a_1, a_2$  are positive constants. Interestingly, a similar divergent behavior of  $\sigma(t)$  for  $t \rightarrow 4m_\pi^2$  is also observed in heavy baryon chiral perturbation theory [18–20]. There this feature arises as a peculiarity of the nonrelativistic expansion and can be avoided by considering baryon chiral perturbation theory in the manifestly Lorentz invariant form [21]. It is not clear whether in the  $\chi$ QSM this unphysical feature could also be cured—possibly by a more careful analytical continuation of  $\sigma(t)$  to  $t > 0$ , e.g., by making use of (subtracted) dispersion relations.

*Accuracy of the approximation.* Before discussing the results let us estimate the size of some of the contributions neglected in Eq. (36). The contribution of the discrete level in Eq. (22) is  $(\sigma_{\pi N})_{lev} = 12 \text{ MeV}$  [62] (cf. next paragraph). The contribution to the continuum part of  $\sigma_{\pi N}$  from the second order of the gradient expansion is  $(\sigma_{\pi N})_{cont}^{(2)} \approx -6 \text{ MeV}$  (cf. Appendix A). These are corrections of  $\mathcal{O}(15\%)$  to Eq. (38), i.e., *smaller* than the theoretical accuracy of the approximation (36) which is  $\mathcal{O}(M^2 \rho_{av}^2) = \mathcal{O}(30\%)$ . This is an

indication (and no more) that the approximation works. Its theoretical justification is anyway unquestioned due to Eq. (8).

*Comparison to previous calculations in the  $\chi$ QSM.* In Refs. [27,28]  $\sigma_{\pi N}$  was studied in SU(2) in leading order of the large- $N_c$  expansion. In Ref. [29] the form factor was studied in the SU(3) version of the model and including  $1/N_c$  corrections. In Refs. [27–29] the proper time regularization was used. Our result (38) for  $\sigma_{\pi N}$  agrees with the numbers quoted in Refs. [27–29] to within 30%.

In Ref. [29] it also was observed that  $\sigma(t)$  is not defined for  $t \geq 4m_\pi^2$ . In the region  $0 < t < 2m_\pi^2$  our result for the difference  $\sigma(t) - \sigma(0)$  agrees with the result of Ref. [29] to within (10–20)%. In the region  $t < 0$  the agreement of the rescaled form factor, i.e.,  $\sigma(t)/\sigma(0)$ , is even more impressive (a few percent). It is not surprising to observe the approximation to work differently in different  $t$  regions. The approximation (36) indicates the limitations of the numerical (finite box) method used in Ref. [29]. From Eqs. (B1),(B2) in Appendix B it is clear that integrals (in coordinate space) converge more and more slowly as  $t$  approaches  $t = 4m_\pi^2$  (from below). In the finite box method, however, it is necessary that integrals converge quickly in order to be in the continuum (box size  $\rightarrow \infty$ ) limit. Therefore in Ref. [29] the region  $t > 2m_\pi^2$  could not be explored and quantitative observations of the kind (43) were not possible.

In Ref. [62] the twist-3 distribution function  $e^a(x)$  and—by exploring the sum rule (19)—also  $\sigma_{\pi N}$  were computed in the  $\chi$ QSM by means of the interpolation formula of Ref. [46]. To remind, the interpolation formula consists in estimating the continuum contribution essentially in the same way we did here, but to add also the exactly evaluated discrete level contribution, which is  $(\sigma_{\pi N})_{\text{lev}} = 12$  MeV. The total result  $\sigma_{\pi N} = 80$  MeV of Ref. [62] agrees with the result (38) obtained here to within 15%.

To summarize, the instanton-motivated approximation for  $\sigma(t)$ , Eq. (36), yields results in agreement with earlier model calculations to within the expected accuracy.

*Comparison to experimental information.* The result  $\sigma(2m_\pi^2) = 83$  MeV in Eq. (39) agrees well with the more recently extracted values of  $\sigma(2m_\pi^2) = (80–90)$  MeV [6–9]. The result for  $\sigma(t) - \sigma_{\pi N}$  in the region  $(-2m_\pi^2) < t < 4m_\pi^2$ , cf. Fig. 1(b), agrees with the result obtained from the dispersion relation analysis with chiral constraints of Ref. [5] to within (2–5)%. This can be seen by comparing the difference  $\Delta_\sigma$  in Eqs. (4),(40) and the slope of  $\sigma(t)$  at  $t=0$ , namely  $\sigma'(0) \propto \sigma_{\pi N} \langle r_S^2 \rangle = 72$  MeV fm<sup>2</sup> of Ref. [5] vs 68 MeV fm<sup>2</sup> obtained here. The agreement with phenomenological information can be considered as satisfactory.

*Comparison to other approaches.* Our result is consistent with the values for  $\sigma_{\pi N}$  obtained from lattice QCD results [23–25] (see also Sec. VI). In Table I we compare our result also to calculations performed in chiral perturbation theory [18,20,21], the linear sigma model [30], Skyrme model [31,32], color-dielectric model [33], cloudy bag model [34,35], Nambu–Jona-Lasinio model [36,37], perturbative chiral quark model [38], a relativistic dynamical model based on effective hadronic ( $N$ ,  $\Delta$ ,  $\pi$ ,  $\rho$ , and  $\sigma$ ) degrees of free-

dom [40]. Also the results of the data analyses and from the  $\chi$ QSM calculations [27,29] are included.

In several models it was observed that a sizable—if not dominant—contribution to  $\sigma_{\pi N}$  is due to the pion cloud (“quark sea”) as compared to the constituent quark core (“valence quarks”) [33–35,38]. In the  $\chi$ QSM the discrete level contribution corresponds to the quark core and the continuum contribution to the pion cloud.<sup>3</sup> Here we obtain an extreme picture, where  $\sigma_{\pi N}$  is purely due to the pion cloud. Corrections to this picture are suppressed by the instanton packing fraction (and are practically of order 30%).

*Skyrmion and nonrelativistic limit.* It is possible to recover from expressions of the  $\chi$ QSM the results of the nonrelativistic quark model and the Skyrme model by taking appropriate (nonphysical) limits [67].

The “Skyrmion limit” consists in taking  $R_{\text{sol}} \rightarrow \infty$ . Since for the soliton solution  $R_{\text{sol}} \approx M^{-1}$  [42], the limit is to be understood as evaluating model quantities with, e.g., the profile in Eq. (13) which allows us to vary  $R_{\text{sol}}$  [67]. In this limit the energy of the discrete level  $E_{\text{lev}} \rightarrow (-M)$  [42], such that this contribution is enclosed in the contour of the  $\omega$  integral in Eq. (25). With increasing  $R_{\text{sol}}$  the contributions  $(\sigma_{\pi N})_{\text{cont}}^{(k)}$  in the series (26) behave as  $(\sigma_{\pi N})_{\text{cont}}^{(k)} \propto R_{\text{sol}}^{3-k}$ . For  $(\sigma_{\pi N})_{\text{cont}}^{(0)}$  and  $(\sigma_{\pi N})_{\text{cont}}^{(2)}$  this can be seen directly from the expressions in the Appendix. For arbitrary  $k$  one arrives at this conclusion using general scaling arguments. Thus  $(\sigma_{\pi N})_{\text{cont}}^{(0)}$  dominates again—this time, however, justified by the unphysical  $R_{\text{sol}} \rightarrow \infty$  limit. The expression for  $\sigma_{\pi N}$  obtained here *formally* coincides with the expressions in Refs. [31,32]. It should be noted that what is an exact result in the Skyrme model is here merely an approximation—though a well justified one thanks to arguments from the instanton vacuum model. The coincidence of the expressions is purely formal since the Skyrmion is a topological soliton. E.g., in Ref. [32] a vector-meson model was used to determine the  $U$  field.

In the opposite limit,  $R_{\text{sol}} \rightarrow 0$ , one recovers results from the nonrelativistic constituent quark model (formulated for arbitrary  $N_c$  [68]). Taking  $R_{\text{sol}} \rightarrow 0$  in the expression (16) one obtains

$$\sigma(t) = M_N G_E(t), \quad (44)$$

where  $G_E(t)$  [normalized to  $G_E(0) = 1$ ] denotes the isoscalar electric form factor—taken also in the nonrelativistic limit. This result follows from generalizing the discussion in Ref. [62] to the case of the form factor  $\sigma(t)$ . That Eq. (44) is the correct nonrelativistic relation between  $\sigma(t) \propto \langle N' | \bar{\psi} \psi | N \rangle$  and  $G_E(t) \propto \langle N' | \psi^\dagger \psi | N \rangle$  follows from considering that in this limit the nucleon wave function has no

<sup>3</sup>This is to be understood in a loose sense in the “quark model language.” Strictly speaking there is no one-to-one correspondence in the  $\chi$ QSM between the discrete level and continuum contributions on the one hand and the notions of “valence” and “sea quarks” on the other hand. The latter are well defined, e.g., in the context of parton distribution functions. The point is that both discrete level and continuum contribute each to valence and sea quark distributions [46,47].

TABLE I. Comparison of the results for  $\sigma_{\pi N}$ ,  $\sigma(2m_\pi^2)$ ,  $\Delta_\sigma \equiv \sigma(2m_\pi^2) - \sigma_{\pi N}$ , and  $\langle r_S^2 \rangle$  from data analyses and theoretical approaches. The list is far from complete, only some of the more recent results are shown. For reviews on early approaches see Ref. [1].

	$\sigma_{\pi N}/\text{MeV}$	$\sigma(2m_\pi^2)/\text{MeV}$	$\Delta_\sigma/\text{MeV}$	$\langle r_S^2 \rangle^{1/2}/\text{fm}$
Data analyses				
Koch (1982) [4]		64 ± 8		
Gasser <i>et al.</i> (1991) [5]	45 ± 8	60 ± 8	15.2 ± 0.4	~ 1.3
Kaufmann and Hite (1999) [6]		88 ± 15		
Olsson (2000) [7]		71 ± 9		
Pavan <i>et al.</i> (2002) [8]		79 ± 7		
Theoretical approaches				
Conventional heavy baryon $\chi$ PT [20]			4 ± 1	
Manifestly Lorentz invariant $\chi$ PT [21]			14	
Lattice QCD, Dong <i>et al.</i> (1995) [23]	49.7 ± 2.6		6.6 ± 0.6	0.72 ± 0.09
Lattice QCD, Leinweber <i>et al.</i> (2000) [24]	45–55			
Lattice QCD, Leinweber <i>et al.</i> (2003) [25]	37 <sup>+35</sup> <sub>-13</sub> –73 <sup>+15</sup> <sub>-15</sub>			
SU(2) $\chi$ QSM to LO $N_c$ [27]	54			
SU(3) $\chi$ QSM to NLO $N_c$ [29]	41	59	18	1.2
Linear sigma model [30]	86–89			
SU(2) Skyrmon [31]	49			
SU(3) Skyrmon [32]	60			
Chiral color dielectric soliton [33]	37.8			1.1
Cloudy bag model [34]	(37–47) ± 9			
Nambu–Jona-Lasinio [36]	50			
Confined Nambu–Jona-Lasinio [37]	60			
Perturbative chiral quark model [38]	45 ± 5			
Effective model of hadrons [40]		74		
This work (accuracy ~ 30%)	67.9	82.6	14.7	1.00

lower (antiquark) component such that  $\psi^\dagger \psi = \bar{\psi} \psi$  practically holds, and that the current quark mass  $m$  has to be understood as a constituent quark mass equal to  $M_N/3$ . The non-relativistic relation  $\sigma_{\pi N} = M_N$  strongly overestimates the phenomenological value of  $\sigma_{\pi N}$  in Eq. (5). Still, this result is theoretically consistent and, e.g., correctly implies a vanishing strangeness content  $y$  in the nucleon [61].

*Interpretation of  $\sigma_{\pi N}$ .* In the effective theory (6) the pion-nucleon sigma term and the quark vacuum condensate are proportional to each other

$$\sigma_{\pi N} \propto -m \langle \bar{\psi} \psi \rangle_{\text{vac}}, \quad (45)$$

up to parametrically small  $\mathcal{O}(M^2 \rho_{\text{av}}^2)$  corrections. From a physical point of view this observation based on Eq. (33) is not surprising since  $\langle \bar{\psi} \psi \rangle_{\text{vac}}$  is the sigma term of the vacuum (per unit volume, up to the explicit factor of  $m$ ). Thus in the  $\chi$ QSM the picture emerges that  $\sigma_{\pi N}$  (measure of chiral symmetry breaking in the nucleon) is directly proportional to

$\langle \bar{\psi} \psi \rangle_{\text{vac}}$  (measure of spontaneous chiral symmetry breaking) and  $m$  (measure of explicit chiral symmetry breaking). The relation (45) is also known from the Skyrme model [31,69] which is not surprising, see the remarks in the previous paragraph.

The proportionality factor in Eq. (45), the function  $B(t)$  at  $t=0$  as defined in Eq. (29), has the dimension of volume. Following the temptation to define “an effective volume of the nucleon” as  $V_{\text{eff}} \equiv B(0)$ , the relation between  $\sigma_{\pi N}$  and  $\langle \bar{\psi} \psi \rangle_{\text{vac}}$  can be written as

$$\sigma_{\pi N} = -m \langle \bar{\psi} \psi \rangle_{\text{vac}} V_{\text{eff}}, \quad V_{\text{eff}} \equiv B(0). \quad (46)$$

Numerically we find an effective volume which—taking the nucleon to be a rigid sphere—would correspond to an effective nucleon radius of 0.9 fm (for  $m_\pi = 140$  MeV). This value should not be taken too seriously. But it yields the

correct order of magnitude for the phenomenological size of the nucleon.  $V_{\text{eff}}$  has a well defined chiral limit, see below. The concept of such an effective volume is useful, e.g., in the context of the “partial restoration of chiral symmetry in nuclear matter.” The  $V_{\text{eff}} \equiv \sigma_{\pi N} / (m_\pi^2 f_\pi^2)$  in Eq. (46) is just the inverse of the chiral nucleon density  $\rho_N^\chi$  introduced in Ref. [10].

Thus the value of  $\sigma_{\pi N}$  is large because  $(-m \langle \bar{\psi} \psi \rangle_{\text{vac}})$  is sizable *and* because the nucleon is a large extended object. Corrections to this picture are suppressed by the instanton packing fraction.

*The strangeness content of the nucleon.* Our result  $\sigma_{\pi N} = 68$  MeV implies a strangeness content in the nucleon of  $y \sim 0.4$ , cf. Sec. II, as it is also inferred from the more recent data analyses [6–9]. In view of such a large value for the strangeness content some authors even suggest to reconsider the “standard interpretation” relating  $\sigma_{\pi N}$  and  $y$  [8]. (However, as argued in Ref. [13]—despite the large strangeness content—the *total* contribution of the strange degree of freedom to the nucleon mass is small.)

The calculation presented in this work definitely confirms—within its accuracy—that  $\sigma_{\pi N}$  is large, and suggests an “explanation” why (“because the nucleon is a large extended object,” see previous paragraph). Being a calculation in a SU(2) model, however, it unfortunately cannot provide any insights into the puzzle why the strangeness content  $y$  appears to be so large. In this context it is worthwhile mentioning that in Ref. [29], where  $\sigma_{\pi N}$  was studied in the SU(3) version of the  $\chi$ QSM and the matrix element  $\langle N | \bar{\psi}_s \psi_s | N \rangle$  directly evaluated, the strangeness content was determined to be  $y \sim 0.3$ .

The numerical result of Ref. [29] does not provide any physical intuition why this value is so large. It would be interesting to see whether the present approach could be extended to the SU(3) sector and provide any insight in this respect. Such a study, however, goes beyond the scope of this work.

## VI. PION MASS DEPENDENCE OF $\sigma_{\pi N}$ AND $M_N$

The result in Eq. (36) allows us to study the form factor  $\sigma(t)$  as a function of  $m_\pi$ , i.e.,  $\sigma(t, m_\pi)$ . Of particular interest is hereby the behavior in the chiral limit which will be investigated first. Maybe more interesting from a phenomenological point of view is the  $m_\pi$  dependence of the nucleon mass  $M_N$  which can be deduced from  $\sigma_{\pi N}(m_\pi)$  by means of the Feynman-Hellmann theorem. The understanding of the correlation between  $M_N$  and  $m_\pi$  is presently of importance for extrapolations of lattice data—which correspond to pion masses of typically  $m_\pi \gtrsim 500$  MeV—to the physical value of the pion mass.

*Leading nonanalytic contributions.* Expanding the result in Eq. (36) around the point  $m_\pi = 0$  we obtain for  $\sigma_{\pi N}(m_\pi)$ ,  $\Delta_\sigma(m_\pi) \equiv \sigma(2m_\pi^2, m_\pi) - \sigma_{\pi N}(m_\pi)$  and the derivative  $\sigma'(0, m_\pi)$  the following results:

$$\sigma_{\pi N}(m_\pi) = a_0 m_\pi^2 - \frac{27}{64\pi} \frac{g_A^2}{f_\pi^2} m_\pi^3 + \dots, \quad (47)$$

$$\Delta_\sigma(m_\pi) = \frac{9}{64\pi} \frac{g_A^2}{f_\pi^2} m_\pi^3 + \dots, \quad (48)$$

$$\sigma'(0, m_\pi) = \frac{9}{256\pi} \frac{g_A^2}{f_\pi^2} m_\pi + \dots, \quad (49)$$

where the constant  $a_0 = (3\sqrt{6}\pi g_A^{3/2}) / (32f_\pi)$  and the dots denote higher-order terms in the limit  $m_\pi \rightarrow 0$  (see Appendix B). Since  $m_\pi^2 \propto m$ , odd powers of  $m_\pi$  in Eqs. (47),(48),(49) are the, respectively, leading nonanalytic contributions in the current quark mass  $m$ . Leading nonanalytic contributions are of particular interest, because they are model independent. The leading nonanalytic contributions in Eqs. (47),(48) are exactly three times larger than those obtained in chiral perturbation theory. The discrepancy is explained by recalling that here we work in the large- $N_c$  limit and that the limits  $N_c \rightarrow \infty$  and  $m_\pi \rightarrow 0$  do not commute [17,70]. In the large- $N_c$  counting  $M_\Delta - M_N = \mathcal{O}(N_c^{-1})$  while  $m_\pi = \mathcal{O}(N_c^0)$  such that it is appropriate to consider first the large- $N_c$  limit, which is done here (though  $M_\Delta - M_N > m_\pi$  in nature would suggest the opposite).  $M_N(m_\pi)$  has a branching point at  $(m_q \propto) m_\pi^2 = (M_\Delta - M_N)^2$  which in the strict large- $N_c$  limit contributes to the nonanalytic behavior of  $M_N(m_\pi)$  at  $m_\pi^2 = 0$ . As a consequence the  $\Delta$  contributes as intermediate state in chiral loops to leading nonanalytic contributions, and its contribution is twice (for isoscalar quantities) that of intermediate nucleon states in the strict large- $N_c$  limit [71].

The result in Eq. (49) means that the scalar isoscalar mean-square radius diverges in the chiral limit

$$\langle r_S^2 \rangle = \left( \frac{27g_A}{32\pi} \right)^{1/2} \frac{1}{m_\pi f_\pi} \cdot \{1 + \mathcal{O}(\text{regular terms})\}. \quad (50)$$

Another example of a square radius which diverges (however, as  $\ln m_\pi$ ) in the chiral limit is the electric isovector charge mean-square radius. (Also this feature is observed in the  $\chi$ QSM [44].)

Interestingly, the correct leading nonanalytic contributions follow here from the structure of the soliton, and not from chiral loops as in chiral perturbation theory. In Ref. [71] it was shown that the leading nonanalytic contribution to  $\sigma_{\pi N}$  in Eq. (47) is a general result in a large class of chiral soliton models of the nucleon. This result is reproduced here in the  $\chi$ QSM because the analytic profile (13) correctly describes the long-distance behavior of the chiral pion field [71].

*Full dependence on  $m_\pi$ .* Since  $\sigma_{\pi N}(m_\pi)$  vanishes in the chiral limit as  $m_\pi^2$  we consider the ratio  $\sigma_{\pi N}(m_\pi)/m_\pi^2$ . Figure 2(a) shows  $\sigma_{\pi N}(m_\pi)/m_\pi^2$  as function of  $m_\pi^2$ . It is preferable to plot  $m_\pi^2$  on the  $x$  axis since the chiral limit corresponds to current quark mass  $m \propto m_\pi^2 \rightarrow 0$ . The solid line shows the full result and the dashed line shows the expansion of  $\sigma_{\pi N}(m_\pi)/m_\pi^2$  in the model up to the leading nonanalytic contribution, Eq. (47). Clearly, only for rather small pion masses  $m_\pi \ll 140$  MeV the full result for  $\sigma_{\pi N}(m_\pi)/m_\pi^2$  is reasonably approximated by its chiral expansion up to the leading nonanalytic contribution in Eq. (47).

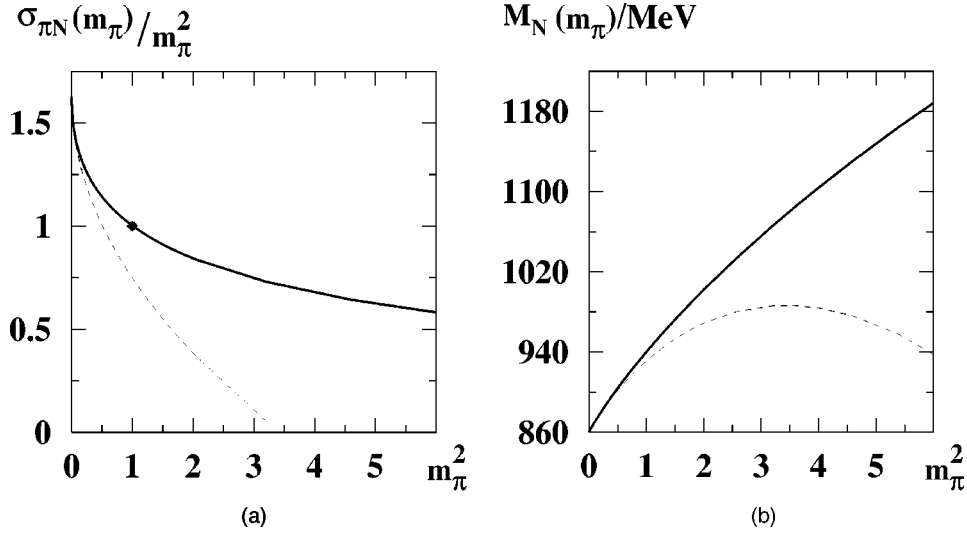


FIG. 2. (a) The ratio  $\sigma_{\pi N}(m_\pi)/m_\pi^2$  as function of  $m_\pi^2$  (with  $m_\pi$  in units of the physical pion mass and  $\sigma_{\pi N}(m_\pi)$  in units of its physical (model) value  $\sigma_{\pi N}=68$  MeV, i.e., the marked point corresponds to the physical situation). The solid line is the full model result, the dashed line is the chiral expansion in the model up to the leading nonanalytic contribution, cf. Eq. (47). (b)  $M_N(m_\pi)$  as function of  $m_\pi^2$  (in units of the physical pion mass). Solid line is the full result, Eq. (52). Dashed line is the (large- $N_c$ ) chiral expansion of  $M_N(m_\pi)$  up to the leading nonanalytic contribution, i.e., Eq. (47) integrated by means of Eq. (51).

Figure 2 simultaneously shows the “effective volume” of the nucleon  $V_{\text{eff}}(m_\pi)$  as defined in Eq. (46) in units of its “physical value” (corresponding to about  $3 \text{ fm}^3$ ). In the chiral limit  $V_{\text{eff}}(m_\pi)$  grows by more than 50% compared to its physical value. But it remains finite which means that this quantity is indeed a useful measure of the “nucleon size” in the chiral limit—in contrast to, e.g., the scalar mean-square radius  $\langle r_S^2 \rangle$ , cf. Eq. (50).

*Nucleon mass as function of  $m_\pi$ .* The Feynman-Hellmann theorem (18), reformulated by means of the Gell-Mann–Oakes–Renner relation in Eq. (34) as

$$\sigma_{\pi N}(m_\pi) = m_\pi^2 \frac{\partial M_N(m_\pi)}{\partial m_\pi^2}, \quad (51)$$

provides a means to study the nucleon mass as function of  $m_\pi$ ,

$$M_N(m_\pi) = M_N(0) + \int_0^{m_\pi^2} d\mu^2 \frac{\sigma_{\pi N}(\mu)}{\mu^2}, \quad (52)$$

where  $M_N(0)$  is an integration constant to be identified with the value of the nucleon mass in the chiral limit.

For the amount the nucleon mass is shifted in the chiral limit with respect to its physical value we obtain from Eq. (52) the result

$$\begin{aligned} M_N(140 \text{ MeV}) - M_N(0) &= \int_0^{m_\pi^2} d\mu^2 \frac{\sigma_{\pi N}(\mu)}{\mu^2} \Bigg|_{m_\pi=140 \text{ MeV}} \\ &= 80 \text{ MeV} \end{aligned} \quad (53)$$

modulo corrections which are parametrically small in the instanton packing fraction. Within this accuracy the mass of

the nucleon in the chiral limit is  $M_N(0)=860$  MeV (taking the physical mass as 940 MeV), which is in the range of the values considered in chiral perturbation theory. Since we work here in the large- $N_c$  limit one obtains the same result for the mass shift of the  $\Delta$  in the (large- $N_c$ ) chiral limit.

Fixing the integration constant  $M_N(0)$  in Eq. (52) to 860 MeV we obtain for  $M_N(m_\pi)$  the result shown in Fig. 2(b), where the solid line shows the full result from Eq. (52) and the dashed line shows the chiral expansion of  $M_N(m_\pi)$  up to the leading nonanalytic contribution, Eqs. (47),(52). Similarly to the case of  $\sigma_{\pi N}(m_\pi^2)$  the chiral expansion up to the leading nonanalytic contribution reasonably approximates the full result for  $M_N(m_\pi)$  only for  $m_\pi$  below the physical pion mass.

Several comments are in order. First, in the  $\chi$ QSM the nucleon mass is given by the minimum of the soliton energy (11) with respect to variations of the chiral field  $U$ . The accurate (and numerically involved) procedure to study the *exact* dependence of  $M_N$  on the pion mass  $m_\pi$  in the  $\chi$ QSM would consist in considering the soliton energy (11) as a function of the current quark mass  $m$  in Eqs. (9),(10) and deducing the respective value of the pion mass from the Gell-Mann–Oakes–Renner relation (34), or the Yukawa-like decay of the self-consistent soliton profile  $\propto \exp(-m_\pi r)/r$  at large  $r$ . Here, however, we can be confident to describe correctly the *variation* of  $M_N$  with  $m_\pi$  to within the accuracy of  $\sigma_{\pi N}$  in Eq. (36).

Next, since Eq. (52) can be used to describe merely the variation of  $M_N$  with  $m_\pi$  it is clear that we are free to choose the integration constant  $M_N(0)=860$  MeV and that there would be no point in taking the precise model value for  $M_N(0)$  which, by the way, would have the drawback of introducing a regularization scheme dependence into the result. It should be noted that in the  $\chi$ QSM the baryon masses tend to be overestimated by about 20% due to spurious contribu-

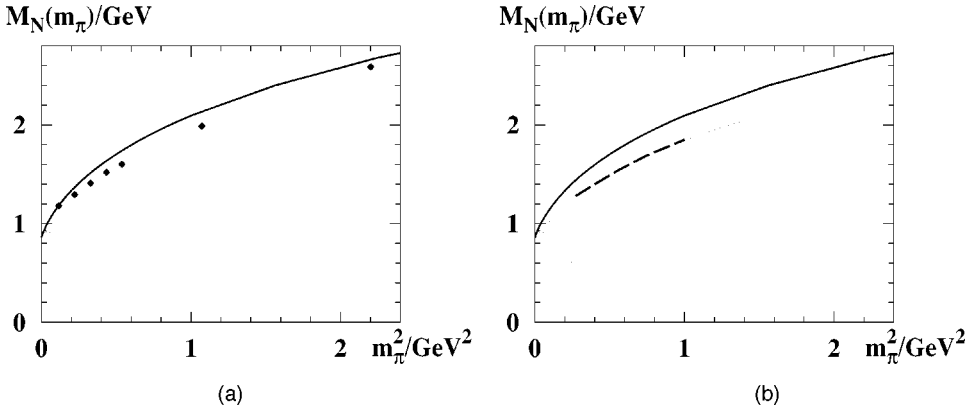


FIG. 3. The nucleon mass  $M_N$  as a function of  $m_\pi^2$  according to Eq. (52) with  $M_N(0) = 860$  MeV in comparison to (a) lattice QCD results from Ref. [73], and (b) from Ref. [74]. (The thick dashed line is actually the fit of Ref. [24] to the lattice results [74].) The meaning of the thin dotted line is explained in the text. In both figures the arrow denotes the physical point.

tions of the center of mass motion of the soliton [72].

Finally, one has to consider that the description of  $M_N(m_\pi^2)$  by means of Eq. (52) can be considered as well justified for  $m_\pi^2 \rho_{\text{av}}^2 \ll 1$ . This relation is analog to Eq. (8) and means that only light pions—light with respect to the scale  $\rho_{\text{av}}^{-1}$ —make sense as effective degrees of freedom in the low-energy theory (6).

Though, of course, it is not their actual goal, lattice QCD simulations allow us to measure  $M_N(m_\pi)$ . The result for  $M_N(m_\pi)$  from Eq. (52) with  $M_N(0) = 860$  MeV is compared to results from lattice QCD simulations from Refs. [73,74] in Figs. 3(a) and (b). [More precisely, what is plotted in Fig. 3(b) as a thick dashed line is the parametrization of the lattice data [74] reported in Ref. [25].]

Keeping in mind the above-mentioned reservations we observe in Fig. 3 a good agreement with the results for the nucleon mass from lattice QCD simulations reported in Refs. [73,74]. A similarly good agreement is observed with the results reported by other lattice groups [75,76].

*Chiral extrapolation of lattice-QCD results.* Eventually one is interested in the chiral extrapolation of lattice data from the currently available region  $500 \text{ MeV} \leq m_\pi \leq \text{several GeV}$  to the physical value of the pion mass. The lattice data on  $M_N(m_\pi)$  are usually fitted to *Ansätze* of the kind  $M_N(m_\pi) = a + bm_\pi^2$  or  $M_N(m_\pi) = a + bm_\pi^2 + cm_\pi^3$  inspired by the chiral expansion of the nucleon mass, often observing that both *Ansätze* are equally acceptable [76]. However, the approximation of  $M_N(m_\pi)$  by its chiral expansion up to the leading nonanalytic term  $\mathcal{O}(m_\pi^3)$  makes sense only at small values of  $m_\pi$  below the physical pion mass—as was emphasized in Ref. [24] [and can also be seen here in Fig. 2(b)].

An interesting extrapolation method was introduced in Ref. [77] where it was suggested to regularize chiral pion loops (which simulate the pion cloud effect) by introducing appropriate regulators (i.e., form factors which simulate the extended structure of the nucleon). This approach not only incorporates the correct chiral behavior, but also reproduces results of the heavy quark effective theory in the limit  $m \propto m_\pi^2 \rightarrow \infty$ . This gives a certain legitimation that also the intermediate  $m_\pi$  region—as explored in lattice QCD calculations—is reasonably described in this approach. The model dependence of this approach was studied in Refs. [24,25] by using different regulators. The thick dashed curve

in Fig. 3(b) is the fit of Ref. [25] to the lattice data [74] in the range  $500 \text{ MeV} \leq m_\pi \leq 1 \text{ GeV}$ . (The thickness of the curve is comparable to the statistical error of the very accurate lattice data of Ref. [74].) The extrapolation from this region to the physical pion mass yields—within the statistical accuracy of the lattice data and depending on the regulator—values for the nucleon mass which cover the region  $(782_{-122}^{+122} \cdot \cdot \cdot 948_{-216}^{+80})$  MeV. This demonstrates the sensitivity to details of the extrapolation of even very accurate lattice data.

The approach of Refs. [24,25,77] basically corresponds to chiral perturbation theory in different regularization schemes. From the point of view of field theory, however, it is unsatisfactory to observe a strong scheme dependence [78]. Considering the complexity of the problem it is important to have further (model independent) constraints. Recently it was reported that chiral perturbation theory is able to describe reliably  $M_N(m_\pi)$  up to  $m_\pi < 600$  MeV using refined regularization techniques [78]. Presently most of the lattice data are beyond that limit, however, a first matching of chiral perturbation theory and lattice results seems to be possible [78].

The results reported in this work also could provide useful—though certainly not model independent—insights into this issue. Indeed, by reasonably fixing the integration constant  $M_N(0)$ , an agreement with lattice data to within the accuracy of the approach is obtained, cf. Figs. 3(a) and (b). This observation suggests that it would be worthwhile attempting to fit lattice data with an *Ansatz* like, e.g.,

$$M_N(m_\pi) = M_N(0)^{\text{fit}} + \int_0^{m_\pi^2} \frac{d\mu^2}{\mu^2} \sigma_{\pi N}(\mu, R_{\text{sol}}^{\text{fit}}). \quad (54)$$

The *Ansatz* (54) corresponds to Eq. (52) where  $M_N(0)$  and the soliton size  $R_{\text{sol}}$  [cf. Eq. (13)] are allowed to be free parameters,  $M_N(0)^{\text{fit}}$  and  $R_{\text{sol}}^{\text{fit}}$ , to be fitted to lattice data. The *Ansatz* (54) is of more general character: It is not only inspired by the  $\chi$ QSM (and the Skyrme model, cf. previous Sec. V) but actually is based on the large  $N_c$  description of the nucleon as a chiral soliton of the pion field [43,59].

The ansatz (54) means that the pion cloud effect—which is responsible for the growth of the nucleon mass with increasing  $m_\pi$ —is modeled by the structure of the soliton. This is conceptually an independent *Ansatz* to consider pion mass

effects than the method of Refs. [24,25,77], and it has, moreover, the advantage of being regularization scheme independent.

In order to illustrate that the *Ansatz* (54) is reasonable note that  $M_N(0)^{\text{fit}} = 780$  MeV and  $R_{\text{sol}}^{\text{fit}} = 0.93R_{\text{sol}}$  fit the lattice data [74] within their statistical accuracy. The *Ansatz* (54) with these parameters—shown in Fig. 3(b) as the thin dotted line in comparison to the fit obtained in Ref. [25]—yields for the physical nucleon mass about 850 MeV which is in the range of the values reported in Ref. [25]. A careful study whether this is the *best* fit and an estimate of its statistical *and* systematic errors both go beyond the scope of this work. The main systematic error in the *Ansatz* (54) is due to the treatment of the  $\Delta$  as a mass generated state to the nucleon in the large- $N_c$  limit and could be estimated following Ref. [71].

## VII. SUMMARY AND CONCLUSIONS

The sigma-term form factor  $\sigma(t)$  of the nucleon was studied in the limit of a large number of colors in the framework of the chiral quark-soliton model ( $\chi$ QSM). The consistency of this field theoretical approach is illustrated by the fact that the pion-nucleon sigma term  $\sigma_{\pi N}$  can consistently be computed in the  $\chi$ QSM in three different ways. Apart from continuing analytically the form factor to  $t=0$  one also can make use of the Feynman-Hellmann theorem [55] and the sum rule for the twist-3 distribution function  $e^a(x)$  [60].

The model expression for  $\sigma(t)$  was evaluated in an approximation justified by arguments from the instanton model of the QCD vacuum from which the  $\chi$ QSM was derived. The approximation is therefore theoretically well controlled and justified. A virtue of the approximation is that it allows us to regularize  $\sigma(t)$ , which is quadratically UV divergent in the  $\chi$ QSM, in a regularization scheme independent way. The theoretical accuracy of the results is governed by the smallness of the parameter characterizing the diluteness of the instanton medium and is practically of  $\mathcal{O}(30\%)$ . Results from previous exact calculations in the  $\chi$ QSM are reproduced to within this accuracy. There are no adjustable parameters in the approach.

For the form factor at the Cheng-Dashen point the value  $\sigma(2m_\pi^2) = 83$  MeV is found—in good agreement with more recent analyses of pion-nucleon scattering data [6–9]. In the region  $-2m_\pi^2 < t < 4m_\pi^2$  the result for the form factor agrees to within a few percent with the shape for  $\sigma(t)$  obtained in Ref. [5] on the basis of a dispersion relation analysis. In particular  $\sigma(2m_\pi^2) - \sigma(0) = 14.7$  MeV is obtained which is close to the value 15.2 MeV of Ref. [5]. Finally, for the pion-nucleon sigma term the value  $\sigma_{\pi N} = 68$  MeV is found.

An advantage of the present approximate result for  $\sigma(t)$  is its simple structure which allows us, e.g., to study the form factor in the chiral limit and to derive the leading nonanalytic (in the current quark mass) contributions in the model. It was shown that the expressions from the  $\chi$ QSM contain the correct leading nonanalytic contributions in the large- $N_c$  limit [71].

The results presented in this work fully confirm the ob-

servation made in other chiral models that the dominant contribution to  $\sigma_{\pi N}$  is due to the pion cloud. Indeed, here the extreme situation emerges that  $\sigma_{\pi N}$  is solely due to the pion cloud—modulo small corrections suppressed by the instanton packing fraction. Moreover, it is found that  $\sigma_{\pi N}$  is proportional to the quark vacuum condensate, i.e., the order parameter characterizing spontaneous chiral symmetry breaking, and to the current quark mass, i.e., the parameter characterizing explicit chiral symmetry breaking—a relation previously known only from the Skyrme model. The proportionality factor can be interpreted as an effective volume of the nucleon, which yields the physically appealing explanation that  $\sigma_{\pi N}$  is so sizeable because the nucleon is a large extended object.

The large value of  $\sigma_{\pi N}$  implies according to the standard interpretation a surprisingly sizeable strangeness content of the nucleon of about  $y \equiv 2\langle N | \bar{\psi}_s \psi_s | N \rangle / \langle N | \bar{\psi}_u \psi_u + \bar{\psi}_d \psi_d | N \rangle \sim 0.4$ . The SU(2) calculation presented here unfortunately cannot shed any light on this puzzle. Calculations in the SU(3) version of the  $\chi$ QSM, however, naturally accommodate a large strangeness content [29]. Worth mentioning in this context is the conclusion [13] that despite the large value of  $y$  the total contribution of strange quarks to the nucleon mass is small.

The dependence of the nucleon mass  $M_N$  on the pion mass was obtained from  $\sigma_{\pi N}(m_\pi)$  by exploring the Feynman-Hellmann theorem. In the chiral limit the nucleon mass was found to be reduced by 80 MeV with respect to its physical value. This means that the mass of the nucleon in the chiral limit is about 860 MeV which is in the range of the values considered in chiral perturbation theory. To within the accuracy of the approach the functional dependence of the nucleon mass on the pion mass agrees with lattice QCD results up to the largest available lattice values of  $m_\pi$ . This observation can be used to inspire *Ansätze* for the chiral extrapolation of lattice QCD results.

Despite the considerable progress of the rigorous approaches to QCD—lattice QCD and the effective-field theory method of chiral perturbation theory—the description of the pion-nucleon sigma term still is a demanding issue. The direct calculation of  $\sigma_{\pi N}$  on the lattice meets the problem that the corresponding operator is not renormalization scale invariant [23]. This complication is avoided by the method of determining  $\sigma_{\pi N}$  from the pion mass dependence of the nucleon mass [73–76]. In either case, however, the conceptual problem appears of how to extrapolate lattice data from the presently available  $m_\pi \gtrsim 500$  MeV down to the physical value of the pion mass. A model-independent guideline can, in principle, be delivered by the chiral perturbation theory where, however, the physical value of  $\sigma_{\pi N}$  cannot directly be computed since it serves to absorb counter terms and is renormalized anew in each order of the chiral expansion.

Recently a first promising matching of chiral perturbation theory to the lowest presently available pion masses in lattice QCD was reported [78]. However, it will take some time to demonstrate and establish the convergence of the chiral expansion up to values of  $m_\pi \sim 500$  MeV and higher. Until then less rigorous but phenomenologically and theoretically

well motivated approaches may have a chance to serve as helpful guidelines for the chiral extrapolation of lattice data. One such approach, suggested in Ref. [77], consists in exploring physically motivated regularization technics to simulate pion cloud effects. In order to investigate the model dependence it would be desirable to consider also other conceptually different approaches.

The observations made in this work inspire an alternative, regularization scheme independent, extrapolation *Ansatz* in which the pion cloud is modelled on the basis of the soliton picture of the nucleon. In view of the success of this picture in describing baryon properties such *Ansätze* appear to be promising. To provide a theoretically well controlled extrapolation *Ansatz* it will, however, be necessary to introduce systematically  $1/N_c$  corrections which is subject to current investigations.

It would be interesting to study also other observables of the nucleon in this way, using arguments from the instanton vacuum model—which not only largely simplifies the calcu-

lations but is crucial, e.g., to allow the derivation of leading nonanalytic contributions in the  $\chi$ QSM. However, it is questionable whether hereby one could obtain also a *phenomenologically* satisfactory description of observables other than quadratically UV divergent, and the only observable of such kind as far as the author is aware of is the scalar form factor.

## ACKNOWLEDGMENTS

The author thanks S. Boffi, K. Goeke, and M.V. Polyakov for fruitful discussions. This work has partly been performed under Contract No. HPRN-CT-2000-00130 of the European Commission.

## APPENDIX A: GRADIENT EXPANSION

By using  $1/(\omega + iH) = (\omega - iH)/(\omega^2 + H^2)$  and  $\hat{H}^2 = \hat{\mathbf{p}}^2 + M^2 + iM \gamma^k (\nabla^k U \gamma_5)(\hat{\mathbf{x}})$  in Eq. (25) we arrive at the series (26) with the  $\sigma(t)_{\text{cont}}^{(k)}$  given by

$$\sigma(t)_{\text{cont}}^{(k)} = mN_c \int \frac{d\omega}{c2\pi i} \text{Sp} \left[ j_0(\sqrt{-t}|\hat{\mathbf{x}}|) \gamma^0 (\omega - i\hat{H}) \frac{1}{\omega^2 + \hat{\mathbf{p}}^2 + M^2} \left( -iM \gamma^k (\nabla^k U \gamma_5)(\hat{\mathbf{x}}) \frac{1}{\omega^2 + \hat{\mathbf{p}}^2 + M^2} \right)^k - (\hat{H} \rightarrow \hat{H}_0) \right]_{\text{reg}}. \quad (\text{A1})$$

In order to evaluate the zeroth-order contribution  $\sigma(t)_{\text{cont}}^{(0)}$  we saturate the functional trace by the complete set of eigenfunctions of the free momentum operator, i.e.,  $\text{Sp}[\dots] \equiv \int [d^3\mathbf{p}/(2\pi)^3] \langle \mathbf{p} | \text{tr} \dots | \mathbf{p} \rangle$  where tr denotes the trace over flavor and Dirac indices. After taking the Dirac trace we obtain

$$\begin{aligned} \sigma(t)_{\text{cont}}^{(0)} &= -mN_c 4M \int d^3\mathbf{x} j_0(\sqrt{-t}|\hat{\mathbf{x}}|) \\ &\times \text{tr}_F \left( \frac{U + U^\dagger}{2} - 1 \right) \int \frac{d\omega}{c2\pi} \\ &\times \int \frac{d^3\mathbf{p}}{(2\pi)^3} \frac{1}{\omega^2 + \mathbf{p}^2 + M^2} \Big|_{\text{reg}}. \quad (\text{A2}) \end{aligned}$$

The “−1” under the flavor trace ( $\text{tr}_F$ ) originates from the vacuum subtraction term. The  $\omega$  integration over the contour  $C$  in Eq. (28) can be replaced by an integration over the real  $\omega$  axis, and we substitute  $\omega \rightarrow p_E^0$  to use the convenient Euclidean space notation. Using  $\text{tr}_F U = \text{tr}_F U^\dagger$  we obtain the result in Eq. (27).

Similarly we obtain for the  $k=1$  term in Eq. (A1)

$$\begin{aligned} \sigma(t)_{\text{cont}}^{(1)} &= \int \frac{d\omega}{c2\pi} \int \frac{d^3\mathbf{p}}{(2\pi)^3} \frac{imN_c M 8g_{ik} p^i}{(\omega^2 + \mathbf{p}^2 + M^2)^2} \\ &\times \int d^3\mathbf{x} j_0(\sqrt{-t}|\mathbf{x}|) \nabla^k \cos P(|\mathbf{x}|) \Big|_{\text{reg}} \\ &= 0, \quad (\text{A3}) \end{aligned}$$

which is zero due to rotational invariance.

The  $k=2$  term in Eq. (A1) yields after a somehow lengthy calculation,

$$\begin{aligned} \sigma(t)_{\text{cont}}^{(2)} &= -\frac{mN_c M}{16\pi^2} \int d^3\mathbf{x} j_0(\sqrt{-t}|\mathbf{x}|) \\ &\times \text{tr}_F U^\dagger(\mathbf{x}) (\nabla^k U)(\mathbf{x}) (\nabla^k U^\dagger)(\mathbf{x}). \quad (\text{A4}) \end{aligned}$$

For our purposes it is sufficient to observe that  $\sigma(t)_{\text{cont}}^{(2)}$  is finite, e.g.,  $(\sigma_{\pi N})_{\text{cont}}^{(2)}/m \leq -(3\sqrt{2}/16)N_c M R_{\text{sol}}$ . [The equality holds for  $m_\pi=0$  in the profile Eq. (13).] Higher orders  $k \geq 3$  are also finite, i.e.,

$$\sigma(t)_{\text{cont}}^{(k)} = \text{UV finite}, \quad k \geq 2. \quad (\text{A5})$$

## APPENDIX B: $\sigma(t)$ AND THE CHIRAL LIMIT

Taking the trace over flavor indices in the expression for  $B(t)$  in Eq. (29) and inserting the result into the expression (36) for  $\sigma(t)$  we obtain for the soliton profile in Eq. (13),

$$\begin{aligned} \sigma(t) &= m_\pi^2 f_\pi^2 4\pi \int_0^\infty dr r^2 j_0(r\sqrt{-t})(1 - \cos P(r)), \\ 1 - \cos P(r) &= \frac{2R_{\text{sol}}^4 (1 + m_\pi r)^2 \exp(-2m_\pi r)}{r^4 + R_{\text{sol}}^4 (1 + m_\pi r)^2 \exp(-2m_\pi r)}. \quad (\text{B1}) \end{aligned}$$

The form factor can be continued analytically to the phenomenologically interesting region  $t \geq 0$  as

$$j_0(r\sqrt{-t}) = \begin{cases} \frac{\sin(r\sqrt{-t})}{r\sqrt{-t}} & t < 0, \\ 1 & t = 0, \\ \frac{\sinh(r\sqrt{t})}{r\sqrt{t}} & t > 0. \end{cases} \quad (\text{B2})$$

The form factor (B1) is undefined for  $t \geq 4m_\pi^2$ . For positive values of  $t$  the integral over  $r$  in Eq. (B1) converges only for  $t < 4m_\pi^2$  because only then at large  $r$  the decay of  $r^2[1 - \cos P(r)] \propto \exp(-2m_\pi r)$  can compensate the rise of  $j_0(r\sqrt{-t}) \propto \exp(r\sqrt{t})/r$ .

*Chiral limit.* The pion-nucleon sigma term  $\sigma_{\pi N}(m_\pi)$  as function of  $m_\pi$  is given by

$$\sigma_{\pi N}(m_\pi) = m_\pi^2 f_\pi^2 2R_{\text{sol}}^3 4\pi I(m_\pi R_{\text{sol}}),$$

$$I(a) \equiv \int_0^\infty \frac{dx x^2 (1+ax)^2 \exp(-2ax)}{x^4 + (1+ax)^2 \exp(-2ax)}. \quad (\text{B3})$$

The zeroth order in the Taylor of the function  $I(a)$  around  $a=0$  is

$$I(0) = \int_0^\infty \frac{dx x^2}{x^4 + 1} = \frac{\pi}{2\sqrt{2}}. \quad (\text{B4})$$

The linear term in the Taylor expansion of  $I(a)$  requires careful treatment. Consider  $a \neq 0$  and introduce an upper limit  $D \gg R_{\text{sol}}$  in the space integral in Eq. (B1). This simulates the “realistic situation” of computing  $\sigma_{\pi N}$  in a finite volume (as it happens in many model calculations and in lattice QCD). Then

$$\begin{aligned} \frac{\partial I(a)}{\partial a} &= -2a \int_0^{D/R_{\text{sol}}} \frac{dx x^8 (1+ax) \exp(2ax)}{[x^4 \exp(2ax) + (1+ax)^2]^2} \\ &= -2 \int_0^{Dm_\pi} \frac{dz z^8 (1+z) \exp(2z)}{[z^4 \exp(2z) + a^4(1+z)^2]^2}, \end{aligned} \quad (\text{B5})$$

where we substituted  $z=ax$  in the second step and used  $a = m_\pi R_{\text{sol}}$ . Taking the continuum limit  $D \rightarrow \infty$  first, and only then  $m_\pi \rightarrow 0$  (apparently these limits do not commute) we arrive at

$$\frac{\partial I(a)^{a \rightarrow 0}}{\partial a} \rightarrow -2 \int_0^\infty dz (1+z) \exp(-2z) = -\frac{3}{2}. \quad (\text{B6})$$

Thus we obtain

$$I(a) = \frac{\pi}{2\sqrt{2}} - \frac{3}{2}a + \mathcal{O}(\text{higher orders in } a). \quad (\text{B7})$$

Inserting the result (B7) into Eq. (B3) and making use of the relation (14) in order to eliminate  $R_{\text{sol}}$  in favor of the pion decay constant  $f_\pi$  and nucleon axial coupling constant  $g_A$  yields the result in Eq. (47). The results in Eqs. (48),(49) follow in an analogous way. It is not possible to proceed with the Taylor expansion of  $I(a)$  to still higher orders of  $a$ . This is possibly due to the fact that the next contribution in the chiral expansion of  $I(a)$  is  $\propto a^2 \ln a$ , as it is in chiral perturbation theory.

- 
- [1] E. Reya, Rev. Mod. Phys. **46**, 545 (1974); R.L. Jaffe, Phys. Rev. D **21**, 3215 (1980).
- [2] J. Gasser and M.E. Sainio, in *Physics and Detectors for DAΦNE: Proceedings, Frascati Physics Series, Vol. 16*, edited by S. Bianco *et al.* (Istituto Naz. Nucl., Frascati, Italy, 1999), pp. 659–668 (hep-ph/0002283); M.E. Sainio, *πN Newsletter* **16**, 138 (2002).
- [3] S. Weinberg, Phys. Rev. Lett. **17**, 616 (1966); T.P. Cheng and R.F. Dashen, *ibid.* **26**, 594 (1971); L.S. Brown, W.J. Pardee, and R.D. Peccei, Phys. Rev. D **4**, 2801 (1971).
- [4] R. Koch, Z. Phys. C **15**, 161 (1982).
- [5] J. Gasser, H. Leutwyler, and M.E. Sainio, Phys. Lett. B **253**, 252 (1991); **253**, 260 (1991).
- [6] W.B. Kaufmann and G.E. Hite, Phys. Rev. C **60**, 055204 (1999).
- [7] M.G. Olsson, Phys. Lett. B **482**, 50 (2000).
- [8] M.M. Pavan, I.I. Strakovsky, R.L. Workman, and R.A. Arndt, *πN Newsletter* **16**, 110 (2002).
- [9] M.G. Olsson and W.B. Kaufmann, *πN Newsletter* **16**, 382 (2002).
- [10] T.D. Cohen, R.J. Furnstahl, and D.K. Griegel, Phys. Rev. C **45**, 1881 (1992).
- [11] M.C. Birse, Acta Phys. Pol. B **29**, 2357 (1998); J. Phys. G **20**, 1537 (1994); Phys. Rev. C **49**, 2212 (1994).
- [12] C.M. Maekawa, J.C. Pupin, and M.R. Robilotta, Phys. Rev. C **61**, 064002 (2000); M.R. Robilotta, *ibid.* **63**, 044004 (2001).
- [13] X.D. Ji, Phys. Rev. Lett. **74**, 1071 (1995).
- [14] T.P. Cheng, Phys. Rev. D **38**, 2869 (1988).
- [15] A. Bottino, F. Donato, N. Fornengo, and S. Scopel, Astropart. Phys. **13**, 215 (2000).
- [16] U. Chattopadhyay, A. Corsetti, and P. Nath, Phys. Rev. D **66**, 035003 (2002).
- [17] J. Gasser, Ann. Phys. (N.Y.) **136**, 62 (1981).
- [18] V. Bernard, N. Kaiser, and U.G. Meissner, Z. Phys. C **60**, 111 (1993).
- [19] B. Borasoy and U.G. Meissner, Phys. Lett. B **365**, 285 (1996); V. Bernard, N. Kaiser, and U.G. Meissner, *ibid.* **389**, 144 (1996); B. Borasoy and U.G. Meissner, Ann. Phys. (N.Y.) **254**, 192 (1997).
- [20] B. Borasoy, Eur. Phys. J. C **8**, 121 (1999).
- [21] T. Becher and H. Leutwyler, Eur. Phys. J. C **9**, 643 (1999).
- [22] Y. Oh and W. Weise, Eur. Phys. J. A **4**, 363 (1999).
- [23] S.J. Dong, J.F. Lagae, and K.F. Liu, Phys. Rev. D **54**, 5496 (1996).

- [24] D.B. Leinweber, A.W. Thomas, and S.V. Wright, Phys. Lett. B **482**, 109 (2000).
- [25] D.B. Leinweber, A.W. Thomas, and R.D. Young, hep-lat/0302020.
- [26] C.A. Dominguez and P. Langacker, Phys. Rev. D **24**, 1905 (1981).
- [27] D. Diakonov, V.Y. Petrov, and M. Praszalowicz, Nucl. Phys. **B323**, 53 (1989).
- [28] M. Wakamatsu, Phys. Rev. D **46**, 3762 (1992).
- [29] H.C. Kim, A. Blotz, C. Schneider, and K. Goeke, Nucl. Phys. **A596**, 415 (1996).
- [30] M.C. Birse, Phys. Rev. D **33**, 1934 (1986); T.S. Aly, J.A. McNeil, and S. Pruess, *ibid.* **60**, 114022 (1999).
- [31] G.S. Adkins and C.R. Nappi, Nucl. Phys. **B233**, 109 (1984).
- [32] J.P. Blaizot, M. Rho, and N.N. Scoccola, Phys. Lett. B **209**, 27 (1988).
- [33] M.C. Birse and J.A. McGovern, Phys. Lett. B **292**, 242 (1992).
- [34] I. Jameson, A.W. Thomas, and G. Chanfray, J. Phys. G **18**, L159 (1992).
- [35] R.E. Stuckey and M.C. Birse, J. Phys. G **23**, 29 (1997).
- [36] V. Bernard, R.L. Jaffe, and U.G. Meissner, Nucl. Phys. **B308**, 753 (1988).
- [37] A.N. Ivanov, M. Nagy, and N.I. Troitskaya, Phys. Rev. C **59**, 451 (1999).
- [38] V.E. Lyubovitskij, T. Gutsche, A. Faessler, and E.G. Drukarev, Phys. Rev. D **63**, 054026 (2001).
- [39] V. Dmitrasinovic and F. Myhrer, Phys. Rev. C **61**, 025205 (2000).
- [40] S. Kondratyuk, Nucl. Phys. **A710**, 329 (2002).
- [41] D.I. Diakonov and V.Y. Petrov, Pis'ma Zh. Eksp. Teor. Fiz. **43**, 57 (1986) [JETP Lett. **43**, 75 (1986)].
- [42] D.I. Diakonov, V.Y. Petrov, and P.V. Pobylitsa, Nucl. Phys. **B306**, 809 (1988).
- [43] E. Witten, Nucl. Phys. **B223**, 433 (1983).
- [44] C.V. Christov *et al.*, Prog. Part. Nucl. Phys. **37**, 91 (1996).
- [45] R. Alkofer, H. Reinhardt, and H. Weigel, Phys. Rep. **265**, 139 (1996).
- [46] D.I. Diakonov *et al.*, Nucl. Phys. **B480**, 341 (1996); Phys. Rev. D **56**, 4069 (1997).
- [47] P.V. Pobylitsa and M.V. Polyakov, Phys. Lett. B **389**, 350 (1996); C. Weiss and K. Goeke, hep-ph/9712447; P.V. Pobylitsa *et al.*, Phys. Rev. D **59**, 034024 (1999); M. Wakamatsu and T. Kubota, *ibid.* **60**, 034020 (1999); K. Goeke *et al.*, Acta Phys. Pol. B **32**, 1201 (2001); P. Schweitzer *et al.*, Phys. Rev. D **64**, 034013 (2001).
- [48] V.Yu. Petrov *et al.*, Phys. Rev. D **57**, 4325 (1998); M. Penttinen, M.V. Polyakov, and K. Goeke, *ibid.* **62**, 014024 (2000); P. Schweitzer *et al.*, *ibid.* **66**, 114004 (2002); **67**, 114022 (2003).
- [49] See, e.g., the following review and references therein: K. Goeke, M.V. Polyakov, and M. Vanderhaeghen, Prog. Part. Nucl. Phys. **47**, 401 (2001).
- [50] M.V. Polyakov, Phys. Lett. B **555**, 57 (2003).
- [51] D. Diakonov, V. Petrov, and M.V. Polyakov, Z. Phys. A **359**, 305 (1997).
- [52] LEP Collaboration, T. Nakano *et al.*, Phys. Rev. Lett. **91**, 012002 (2003); DIANA Collaboration, V.V. Barmin *et al.*, Yad. Fiz. **66**, 1763 2003 [Phys. At. Nucl. **66**, 1715 (2003)]; CLAS Collaboration, V. Kubarovsky and S. Stepanyan hep-ex/0307088; CLAS Collaboration, S. Stepanyan *et al.*, Phys. Rev. Lett. **91**, 252001 (2003); SAPHIR Collaboration, J. Barth *et al.*, hep-ex/0307083; A.E. Asratyan, A.G. Dolgolenko, and M.A. Kubantsev, hep-ex/0309042.
- [53] D.I. Diakonov and V.Y. Petrov, Nucl. Phys. **B245**, 259 (1984).
- [54] D. Diakonov and V.Y. Petrov, Nucl. Phys. **B272**, 457 (1986).
- [55] H. Hellmann, *Einführung in die Quantenchemie* (Deuticke Verlag, Leipzig, 1937); R.P. Feynman, Phys. Rev. **56**, 340 (1939).
- [56] J. Gasser and H. Leutwyler, Phys. Rep. **87**, 77 (1982).
- [57] D. Diakonov and M.I. Eides, Pisma Zh. Eksp. Teor. Fiz. **38**, 358 (1983) [JETP Lett. **38**, 433 (1983)].
- [58] A. Dhar, R. Shankar, and S.R. Wadia, Phys. Rev. D **31**, 3256 (1985).
- [59] G.S. Adkins, C.R. Nappi, and E. Witten, Nucl. Phys. **B228**, 552 (1983).
- [60] R.L. Jaffe and X.D. Ji, Phys. Rev. Lett. **67**, 552 (1991); **67**, 527 (1991).
- [61] A.V. Efremov and P. Schweitzer, J. High Energy Phys. **08**, 006 (2003).
- [62] P. Schweitzer, Phys. Rev. D **67**, 114010 (2003).
- [63] M. Wakamatsu and Y. Ohnishi, Phys. Rev. D **67**, 114011 (2003).
- [64] S. Kahana and G. Ripka, Nucl. Phys. **A429**, 462 (1984).
- [65] J. Baacke and H. Sprenger, Phys. Rev. D **60**, 054017 (1999).
- [66] T. Kubota, M. Wakamatsu, and T. Watabe, Phys. Rev. D **60**, 014016 (1999).
- [67] M. Praszalowicz, A. Blotz, and K. Goeke, Phys. Lett. B **354**, 415 (1995).
- [68] G. Karl and J.E. Paton, Phys. Rev. D **30**, 238 (1984).
- [69] J.F. Donoghue and C.R. Nappi, Phys. Lett. **168B**, 105 (1986).
- [70] R.F. Dashen, E. Jenkins, and A.V. Manohar, Phys. Rev. D **49**, 4713 (1994); **51**, 2489(E) (1995).
- [71] T.D. Cohen and W. Broniowski, Phys. Lett. B **292**, 5 (1992).
- [72] P.V. Pobylitsa, E. Ruiz Arriola, T. Meissner, F. Grummer, K. Goeke, and W. Broniowski, J. Phys. G **18**, 1455 (1992).
- [73] C.W. Bernard *et al.*, Phys. Rev. D **64**, 054506 (2001).
- [74] CP-PACS Collaboration, A. Ali Khan *et al.*, Phys. Rev. D **65**, 054505 (2002).
- [75] CSSM Lattice Collaboration, J.M. Zanotti *et al.*, Phys. Rev. D **65**, 074507 (2002).
- [76] CP-PACS Collaboration, S. Aoki *et al.*, Phys. Rev. D **60**, 114508 (1999); **67**, 034503 (2003).
- [77] D.B. Leinweber, A.W. Thomas, K. Tsushima, and S.V. Wright, Phys. Rev. D **61**, 074502 (2000); R.D. Young, D.B. Leinweber, A.W. Thomas, and S.V. Wright, *ibid.* **66**, 094507 (2002).
- [78] V. Bernard, T.R. Hemmert, and U.G. Meissner, hep-ph/0307115.